Please cite this article in press as: Radonjić et al., The Dynamic Range of Human Lightness Perception, Current Biology (2011), doi:10.1016/j.cub.2011.10.013

Current Biology *21*, 1–6, November 22, 2011 ©2011 Elsevier Ltd All rights reserved DOI 10.1016/j.cub.2011.10.013

Report

The Dynamic Range of Human Lightness Perception

Ana Radonjić,[1,*] Sarah R. Allred,[2] Alan L. Gilchrist,[3] and David H. Brainard[1]
[1]Department of Psychology, University of Pennsylvania, Philadelphia, PA 19104, USA
[2]Department of Psychology, Rutgers University, Camden, NJ 08102, USA
[3]Department of Psychology, Rutgers University, Newark, NJ 07102, USA

Summary

Natural viewing challenges the visual system with images that have a dynamic range of light intensity (luminance) that can approach 1,000,000:1 and that often exceeds 10,000:1 [1, 2]. The range of perceived surface reflectance (lightness), however, can be well approximated by the Munsell matte neutral scale (N 2.0/ to N 9.5/), consisting of surfaces whose reflectance varies by about 30:1. Thus, the visual system must map a large range of surface luminance onto a much smaller range of surface lightness. We measured this mapping in images with a dynamic range close to that of natural images. We studied simple images that lacked segmentation cues that would indicate multiple regions of illumination. We found a remarkable degree of compression: at a single image location, a stimulus luminance range of 5,905:1 can be mapped onto an extended lightness scale that has a reflectance range of 100:1. We characterized how the luminance-to-lightness mapping changes with stimulus context. Our data rule out theories that predict perceived lightness from luminance ratios or Weber contrast. A mechanistic model connects our data to theories of adaptation and provides insight about how the underlying visual response varies with context.

Results

At the core of any theory of surface lightness perception is a characterization of how luminances in the retinal image are mapped onto percepts that range from black through gray to white. Because the dynamic range of natural images (which can approach 1,000,000:1) vastly exceeds the dynamic range of reflectance scales that describe perceptual lightness (e.g., fresh snow reflects about 80% of the incident light across the visible spectrum, whereas black shingles or black rich soil reflect approximately 4% [3] for a reflectance ratio of 20:1), the mapping cannot be accomplished by a multiplicative scaling of luminance onto lightness. Theories of lightness account for this observation by noting that image luminance is affected both by object surface reflectance and by the intensity of the illuminant, and that the visual system contains mechanisms that discount the variation introduced by the illuminant [4–7]. Such theories divide the research program of understanding lightness into two parts. First, how is luminance mapped to lightness within an image region that is uniformly illuminated? Second, how does the visual system parse the image into regions that share common illumination, and how does information from multiple such regions interact (if at all)? Here we report fundamental measurements that address the first part of this program: our data characterize the luminance-to-lightness mapping in high-dynamic-range images that lack cues indicating the presence of multiple regions of illumination. Our measurements probe the limits of the mechanisms that underlie lightness perception and address key questions about their function.

In experiment 1, observers viewed a 5 × 5 grayscale checkerboard, consisting of homogeneous squares that varied in luminance over a range that we estimate to be greater than 10,000:1 and presented on a high-dynamic-range display (Figure 1). The center square of the 5 × 5 checkerboard served as a test stimulus. The remaining 24 squares varied in luminance over the stimulus range in equal log steps. On each trial, the test square took on the luminance value of one of the surrounding contextual squares. Observers matched lightness of the test by selecting a sample from an extended Munsell neutral palette (N 0.5/ to N 9.5/ in 0.5 value steps). Observers also had the option of responding with three out-of-range judgments: "darker than 0.5," "lighter than 9.5, but still a surface," or "glowing." Experimental protocols were approved by the institutional review board at the University of Pennsylvania.

The measured luminance-to-lightness matching function, shown in Figure 2, exhibits remarkable compression. When viewed in the unsegmented high-dynamic-range context, a luminance range of 5,905:1 was mapped onto a reflectance range of 100:1. Our data falsify a key implication of Wallach's ratio principle [8] and of theories that base perceived lightness on Weber contrast, namely that to match any pair of test patches in a region of uniform illumination, a human observer will select two chips from the palette that stand in the same luminance ratio to each other as the tests.

In experiment 2, we measured the luminance-to-lightness matching function for contextual checkerboards that varied in their photometric properties: the contextual luminance range (that is, luminance ratio between the lowest and the highest contextual square), the overall contextual luminance, and the distribution of contextual luminances when the highest and lowest luminances were held fixed.

Figure 3A plots the matching function for three dynamic range conditions (~10,000:1, ~1,000:1, and ~30:1) across which the highest contextual luminance was held approximately constant. The data for the 10,000:1 checkerboard replicate the results of experiment 1, for different observers and a different spatial arrangement of the checkerboard. The data for the other two checkerboards show that the luminance-to-lightness mapping depends strongly on the contextual range. For example, the luminance range mapped onto the reflectance scale between N 2.5/ and N 9.5/ (the palette range used in common by observers across all three contexts) varied by 1.3 log units across the three dynamic range conditions (see Table S1 available online). Across this large variation, however, the white point (i.e., the luminance matched to N 9.5/) was approximately constant. In addition, the white point was close

*Correspondence: radonjic@sas.upenn.edu

Please cite this article in press as: Radonjić et al., The Dynamic Range of Human Lightness Perception, Current Biology (2011), doi:10.1016/j.cub.2011.10.013

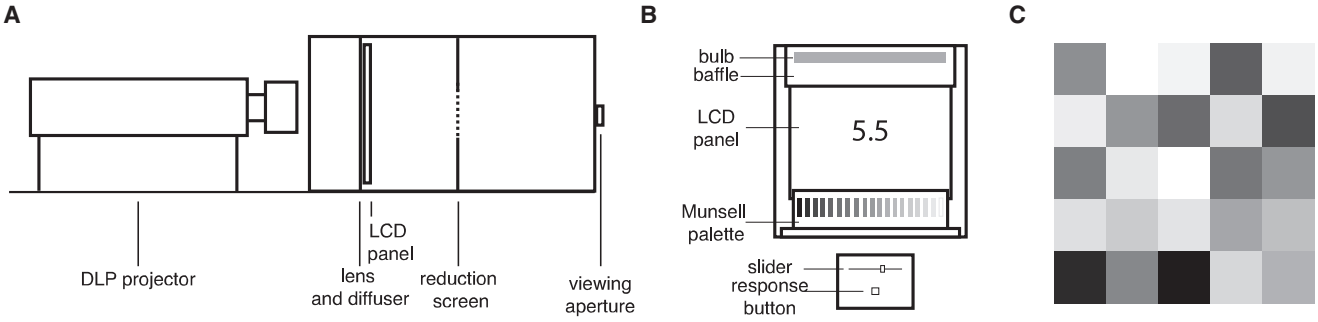

Figure 1. Apparatus

(A) Schematic view of the high-dynamic-range display. A DLP projector projects an image onto an LCD display panel through a Fresnel lens and diffuser, placed directly against the backside of the panel. Because the LCD panel is a transmissive display, it provides a multiplicative attenuation of the projector image, resulting in an overall dynamic range that is nominally the product of the native dynamic ranges of the projector and panel. The observer viewed the resulting image monocularly through an aperture and a reduction screen. The dotted portion of the reduction screen in the diagram shows the vertical extent of a square aperture in that screen. The display is built following the design by Seetzen et al. [43]; details on its calibration are available in [44].

(B) The matching chamber was diffusely illuminated by a fluorescent bulb and contained a matching palette. The palette consisted 19 glossy papers ranging from Munsell N 0.5/ to N 9.5/. A baffle prevented light from the bulb from reaching the observer directly. Observers matched the test square, presented in the center of a checkerboard, to one of the palette papers. They indicated their response using a slider on a custom response box (shown below chamber in diagram). The slider varied a number displayed on an LCD panel mounted at the back of the viewing chamber. Out-of-range response options were displayed as text on the same monitor.

(C) The stimulus was a 5 × 5 checkerboard. The checker squares had Commission Internationale de l'Eclairage (CIE) chromaticity x = 0.309, y = 0.338 and varied in luminance. The test, which was the center square of the checkerboard, took on 24 different luminances during each block of trials. For more details, see Supplemental Experimental Procedures.

to the highest contextual luminance (Table S1) in all conditions, broadly consistent with a "highest luminance appears white" anchoring rule [4, 9]. The agreement is not perfect, however. For example, analysis of the out-of-range judgments (Table S2) shows that the highest luminance test, which matched the highest contextual luminance, was judged glowing on most trials in the 10,000:1 and 1,000:1 contexts. It may be that the minor deviations from the "highest luminance appears white" anchoring resulted from the fact that our stimuli were presented on an emissive display, and thus that the perceptual interpretation of the stimuli as surfaces was imperfect.

We also measured the effect of varying the overall contextual luminance for the 1,000:1 and 30:1 range conditions. In essence, we scaled all contextual and test luminances by a common multiplicative factor (see "Checkerboard Stimulus" in Supplemental Experimental Procedures for luminance values). Figures 3B and 3C show that this manipulation has a simple effect: the luminance-to-lightness matching function shifted by close to the same factor as the stimuli. In particular, perceptual white remained anchored close to the highest contextual luminance, and the shape of the matching functions on the log-log plots was invariant. Subtle effects of overall luminance variation are reflected in the distribution of out-of-range judgments (Table S2).

The final measurements of experiment 2 studied the effect of varying the distribution of contextual luminances while holding the lowest two and highest two contextual luminances constant. The results (Figure 3D) show that this manipulation has little effect on the white point or the luminance range of the matching function but substantially affects the matching function's shape.

We developed a mechanistic model that describes our measured luminance-to-lightness matching functions. We built on models developed in the literature on visual adaptation, which are formulated primarily to account for measurements of visual thresholds [10]. The key idea is that the visual system has a limited response range, described by a saturating response function. The response function varies with context through the action of a small set of adaptation parameters. We combined this idea with the Fechnerian notion that perceived lightness is related to the response by a fixed context-independent transformation, with higher responses corresponding to greater perceived lightness [11–14]. Thus, two tests, each seen in its own context, are predicted to match in lightness if they both produce the same response. The model captures contextual effects on the luminance-to-lightness mapping entirely through changes in the adaptation parameters with context.

We characterized the relation between stimulus luminance L and visual response R using a modified Naka-Rushton function [15]

$$R = \frac{(g(L-c))^n}{(g(L-c))^n + 1}.$$

Three adaptation parameters control the behavior of this function: a multiplicative gain parameter g and a subtractive offset parameter c (which both modify the input to the standard Naka-Rushton function) and an exponent n (which controls the shape of the function). For any choice of adaptation parameters, the response increases from 0 to 1 as a function of luminance. The Supplemental Experimental Procedures describe how the model was fit to the data.

The lines through the data shown in Figure 2 and Figure 3 show the model predictions. The model fits the data well for all experiments and contexts. Figure 4 shows the visual response functions derived from the model. These provide additional insight. First, for all contexts, the upper end of the response functions is located near the highest luminance of the surrounding checkerboard. This is the response function manifestation of the "highest luminance appears white" anchoring rule. Second, as the range of the contextual stimuli increases, the slope of the response function becomes

Please cite this article in press as: Radonjić et al., The Dynamic Range of Human Lightness Perception, Current Biology (2011), doi:10.1016/j.cub.2011.10.013

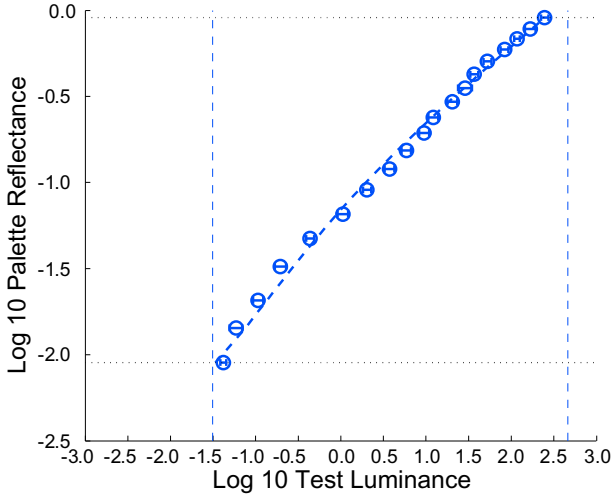

Figure 2. Luminance-to-Lightness Mapping Shows High Compression

Palette log10 reflectance plotted against test log10 luminance (cd/m^2) for experiment 1. Open circles plot the average test luminance for which that paper was chosen as a match, averaged across observers (n = 8); error bars indicate ±1 between-observers standard error of the mean (SEM). Dashed vertical lines show upper and lower limits of contextual/test luminances. Dotted horizontal lines show the minimum and maximum palette paper reflectance. The line through the data shows the fit of the model described in the text. Figure S1 shows that similar results are obtained when a standard Munsell palette (N2.0/ to N 9.5/) is used.

shallower, so that the available response range is allocated to approximately match the luminances in the checkerboard context (Figure 4A). Third, scaling the overall contextual luminance while keeping its range constant simply shifts the response function, so that the response range remains matched to the contextual luminance (Figures 4B and 4C). Finally, when the range of the contextual stimuli is held constant, the visual response function changes so that a larger portion of the response range is allocated to stimulus luminances that occur most often in the checkerboard (Figure 4D). The latter three behaviors are consistent with the general notion that adaptation serves to optimize the use of available response range [16–19].

Discussion

Our measurements provide a foundation for future work that considers more natural contextual images in which segmentation cues cause the luminance-to-lightness mapping to vary from one image region to another. For example, a luminance value that is perceived as black in a region of high illumination might be perceived as white in a region of low illumination [20, 21]. This is consistent with theories of lightness [7, 22, 23] that suggest that the visual system relies on segmentation cues in (e.g., depth boundaries, penumbrae) to stabilize the mapping between object reflectance and perceived lightness. Although our measurements do not speak directly to the effect of such cues, we can now proceed to ask questions such as (1) whether variation in adaptation parameters that we identified can describe luminance-to-lightness mapping functions in high-dynamic-range images that are segmented into differentially illuminated regions and (2) if so, whether the parameters are set by the local within-illuminant context, by the global context, or by some combination of both (for theoretical overviews, see [6, 7, 11]). We have conducted initial experiments along these lines, where photometric cues are available for segmentation (unpublished data).

It may seem surprising that the visual system can maintain a lightness scale over a luminance range that exceeds 5,000:1 at a single image location, because this is much larger than is necessary to perceive variation in surface reflectance. Perhaps the excess operating range serves to preserve useful representations of surface lightness in the face of failures in image segmentation according to illuminant or to handle bright specular highlights on glossy objects. Or perhaps it is a side effect of the early visual system's need to not only represent surface lightness but also preserve discriminability of image luminances (see [19]). It will be of interest to understand how the effects that we report come into play in high-dynamic-range images that can be segmented into separate regions, each of which has a low dynamic range.

The adaptation model that we developed to describe contextual variation in the luminance-to-lightness mapping function provides a connection between two traditions, one that studies the functional characteristics of lightness perception and whose goal is to relate perceived lightness to the visual stimulus, and a second that uses threshold psychophysics and physiological measurements to identify and characterize mechanisms that mediate visual processing. We are not the first to develop adaptation models to account for judgments of appearance, however, and our model incorporates ideas available in the literature. There is ample evidence of the need for an adaptation parameter to describe some form of multiplicative gain control [10]. Our data clearly require additional adaptation parameters: if the only effect of context were to change a multiplicative gain, then the luminance-to-lightness matching functions would all have the same shape on the log-log plots and would differ only in their horizontal positions.

The need for an additional adaptation parameter has been noted previously by numerous authors using a variety of experimental stimuli, methods, and terminologies [7, 24–36]. Our second adaptation parameter, the subtractive offset c, is an instantiation of this second parameter. In addition, we found that a third adaptation parameter, the exponent n, was required to fit our data. When this parameter was held fixed, there were systematic deviations between the model predictions and the data.

Our model allows lightness measurements to generate mechanistic hypotheses that can be explicitly tested. For example, if early mechanisms of adaption mediate our results, the model predicts the way in which the corresponding physiologically measured luminance-response functions should vary with high-dynamic-range contexts. In addition, understanding the parametric form of the luminance-to-lightness matching functions should be useful for refining algorithms designed to render high-dynamic-range images on low-dynamic-range displays [37, 38].

The model in its current form does not provide a complete theory of lightness, because it does not specify how context sets the adaptation parameters. To understand context effects, our strategy was to first determine the parameters that vary with context, as we have done here, and then proceed toward understanding how those parameters are set [39–42]. The regularities in our data suggest that simple rules may suffice for this purpose. Testing the generality of these rules, both for simple checkerboards and for more complex stimuli, will be of considerable interest.

Please cite this article in press as: Radonjić et al., The Dynamic Range of Human Lightness Perception, Current Biology (2011), doi:10.1016/j.cub.2011.10.013

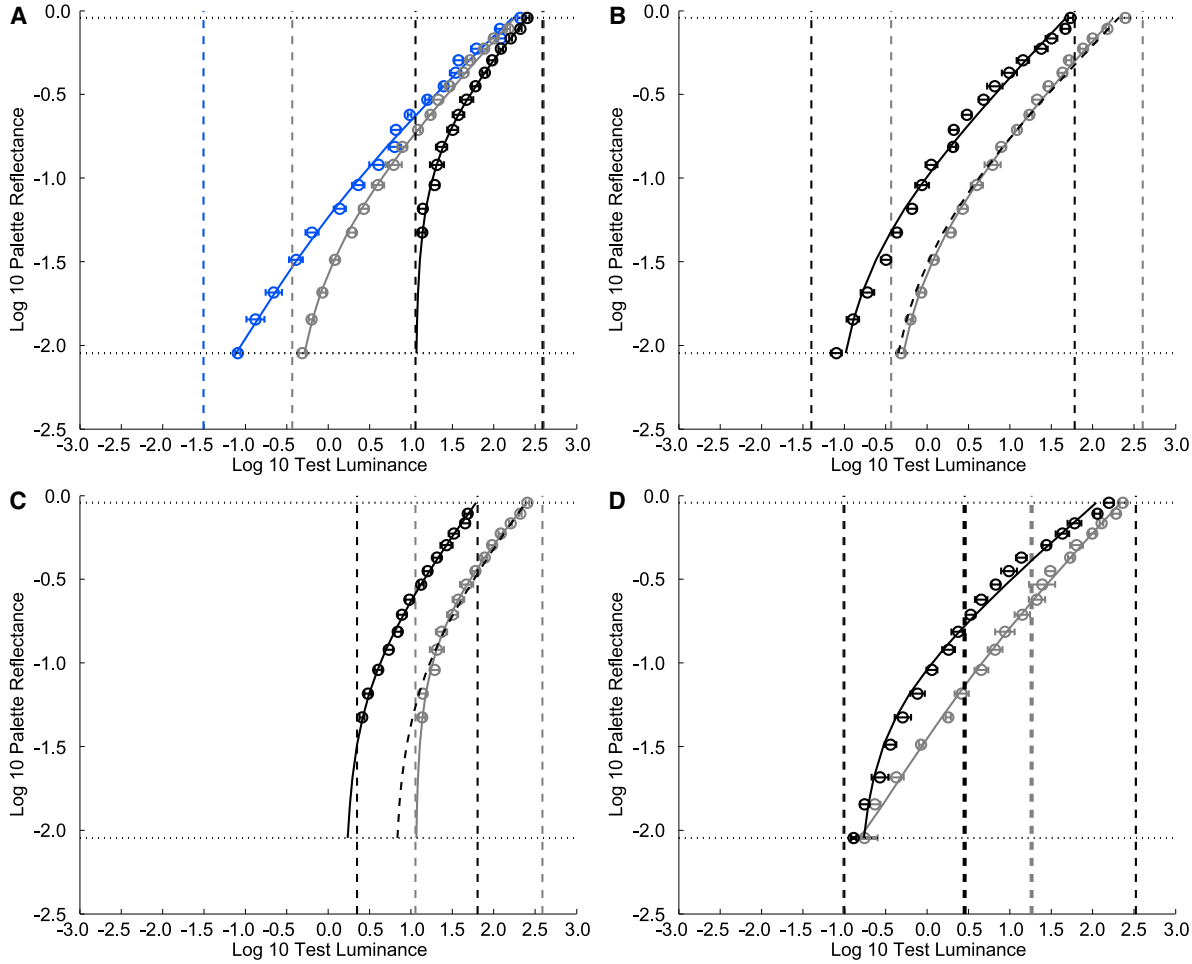

Figure 3. Luminance-to-Lightness Mapping Varies with Context in Experiment 2

All panels have same basic format as Figure 2 (n = 5). Error bars indicate ±1 SEM computed across observers.

(A) Luminance-to-lightness matching functions for three contextual luminance ranges from 10,000:1 (blue), 1,000:1 (gray), and 30:1 (black).

(B) Luminance-to-lightness matching functions for 1,000:1 luminance range context. Solid lines plot the model fits to each overall luminance condition. The dashed line through the high-luminance-condition data shows a shifted version of the fit for the low-luminance condition. The overall contextual luminance change was 0.8 log units. The shift in model fit from high to low overall contextual luminance condition is 0.64 log units. In (B) and (C), the gray points and fit are replotted from (A).

(C) Data for the 30:1 range condition, same format as (B). The overall contextual luminance change was 0.72 log units. The shift in model fit from high to low overall contextual luminance condition is 0.6 log units.

(D) Luminance-to-lightness matching functions for two contexts that had the same lowest two and highest two luminances but a different luminance distribution. Low mean luminance is plotted in black and high mean luminance in gray. Thick dashed vertical lines in corresponding colors represent the contextual mean luminance level for the two contextual configurations (center square excluded).

Figure S2 connects our measurements to classic results obtained with uniform surrounds.

We measured the mapping of stimulus luminance onto perceptual lightness in high-dynamic-range images. We found that the visual system can maintain a lightness scale over more than 3 log units of luminance, considerably larger than is necessary to represent variation in natural surface reflectance. The large degree of compression revealed by our data rules out theories that predict perceived lightness from luminance ratios or Weber contrast. In addition, the luminance-to-lightness mapping depends on the image context. For our experimental images, which contained no cues that would allow segmentation of the image into separate regions of illumination, we found three regularities that described this dependence. First, perceptual white is anchored near the highest luminance in the contextual image, across variations of highest luminance and contextual image luminance range. Second, varying the contextual image luminance range while holding the highest luminance fixed has its primary effect on the range of luminances mapped between perceptual white and perceptual black. Third, changing the distribution of contextual image luminances while holding the highest luminance and luminance range fixed left the luminances mapped to white and black unchanged but affected the shape of the matching function in a manner broadly consistent with theories of optimal image coding. We accounted for the contextual effects using a model based on the adaptation of an underlying visual response function and used the model to derive the response function for each of our experimental contexts.

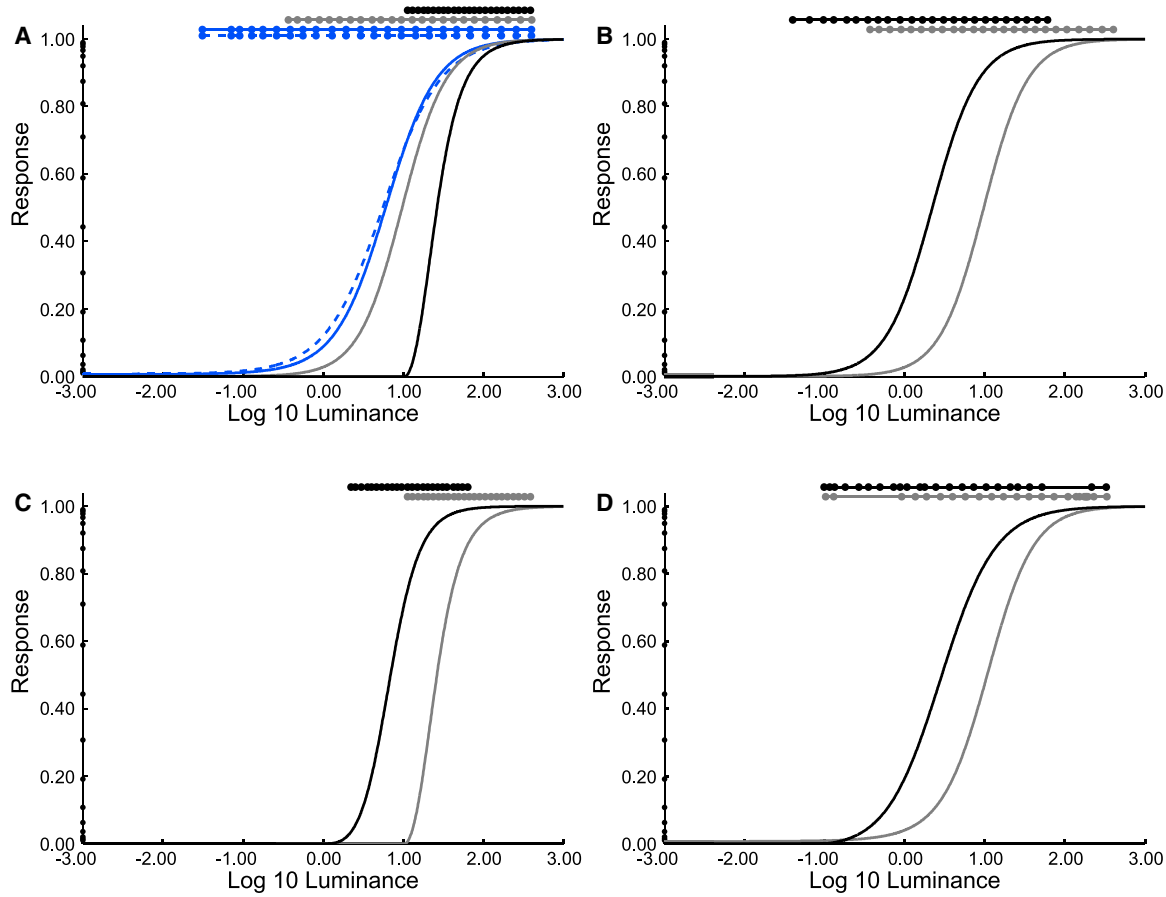

Figure 4. Inferred Response Functions Shift to Match Contextual Luminance Distributions

(A) Response functions inferred from data shown in Figure 2 and Figure 3A. Response is plotted against log test luminance (cd/m^2). The solid dots on the y axis indicate the response corresponding to each palette paper. The bars above the plots indicate the contextual stimulus range for each condition, and the solid dots on these bars indicate the 24 contextual luminances. The dashed blue line represents experiment 1. The solid lines represent experiment 2 and use the same color code as Figure 3.

(B) Response functions inferred from data in Figure 3B.

(C) Response functions inferred from data in Figure 3C.

(D) Response functions inferred from data in Figure 3D.

Supplemental Information

Supplemental Information includes Supplemental Results, three figures, five tables, and Supplemental Experimental Procedures and can be found with this article online at doi:10.1016/j.cub.2011.10.013.

Acknowledgments

This work was supported by National Institutes of Health (NIH) grants RO1 EY10016, RO1 EY10016S1, and P30 EY1001583 (D.H.B.) and by National Science Foundation grant BCS 1027093 and NIH grant 1R25GM096161-01 (A.L.G.). We thank Christopher Broussard for technical assistance.

Received: August 10, 2011
Revised: October 10, 2011
Accepted: October 11, 2011
Published online: November 10, 2011

References

1. Heckaman, R.L., and Fairchild, M.D. (2009). Jones and Condit redux in high dynamic range color. In Seventeenth Color Imaging Conference: Color Science and Engineering Systems, Technologies, and Applications (Springfield, VA: IS&T: The Society for Imaging Science and Technology), pp. 8–14.
2. Xiao, F., DiCarlo, J., Catrysse, P., and Wandell, B. (2002). High dynamic range imaging of natural scenes. In Tenth Color Imaging Conference: Color Science, Systems, and Applications (Springfield, VA: IS&T: The Society for Imaging Science and Technology), pp. 337–342.
3. Wyszecki, G., and Stiles, W.S. (1982). Color Science: Concepts and Methods, Quantitative Data and Formulae, Second Edition (New York: John Wiley & Sons).
4. Land, E.H., and McCann, J.J. (1971). Lightness and retinex theory. J. Opt. Soc. Am. *61*, 1–11.
5. Arend, L.E., and Goldstein, R. (1987). Simultaneous constancy, lightness, and brightness. J. Opt. Soc. Am. A *4*, 2281–2285.
6. Adelson, E.H. (2000). Lightness perception and lightness illusions. In The New Cognitive Neurosciences, Second Edition, M. Gazzaniga, ed. (Cambridge, MA: MIT Press), pp. 339–351.
7. Gilchrist, A. (2006). Seeing Black and White (Oxford: Oxford University Press).
8. Wallach, H. (1948). Brightness constancy and the nature of achromatic colors. J. Exp. Psychol. *38*, 310–324.
9. Gilchrist, A., Kossyfidis, C., Bonato, F., Agostini, T., Cataliotti, J., Li, X., Spehar, B., Annan, V., and Economou, E. (1999). An anchoring theory of lightness perception. Psychol. Rev. *106*, 795–834.
10. Walraven, J., Enroth-Cugell, C., Hood, D.C., MacLeod, D.I.A., and Schnapf, J.L. (1990). The control of visual sensitivity: Receptoral and postreceptoral processes. In Visual Perception: The Neurophysiological

Please cite this article in press as: Radonjić et al., The Dynamic Range of Human Lightness Perception, Current Biology (2011), doi:10.1016/j.cub.2011.10.013

Foundations, L. Spillmann and J.S. Werner, eds. (San Diego, CA: Academic Press), pp. 53–101.
11. Fechner, G.T. (1860). Elemente der Psychophysik (Leipzig, Germany: Breitkopf & Härtel).
12. Nachmias, J., and Steinman, R.M. (1965). Brightness and discriminability of light flashes. Vision Res. *5*, 545–557.
13. Hillis, J.M., and Brainard, D.H. (2007). Do common mechanisms of adaptation mediate color discrimination and appearance? Contrast adaptation. J. Opt. Soc. Am. A Opt. Image Sci. Vis. *24*, 2122–2133.
14. Hillis, J.M., and Brainard, D.H. (2007). Distinct mechanisms mediate visual detection and identification. Curr. Biol. *17*, 1714–1719.
15. Naka, K.I., and Rushton, W.A. (1966). S-potentials from colour units in the retina of fish (Cyprinidae). J. Physiol. *185*, 536–555.
16. Brenner, N., Bialek, W., and de Ruyter van Steveninck, R. (2000). Adaptive rescaling maximizes information transmission. Neuron *26*, 695–702.
17. Grzywacz, N.M., and Balboa, R.M. (2002). A Bayesian framework for sensory adaptation. Neural Comput. *14*, 543–559.
18. von der Twer, T., and MacLeod, D.I.A. (2001). Optimal nonlinear codes for the perception of natural colours. Network *12*, 395–407.
19. Abrams, A.B., Hillis, J.M., and Brainard, D.H. (2007). The relation between color discrimination and color constancy: when is optimal adaptation task dependent? Neural Comput. *19*, 2610–2637.
20. Gilchrist, A.L. (1980). When does perceived lightness depend on perceived spatial arrangement? Percept. Psychophys. *28*, 527–538.
21. Radonjić, A., Todorović, D., and Gilchrist, A. (2010). Adjacency and surroundedness in the depth effect on lightness. J. Vis. *10*, 12.
22. Koffka, K. (1935). Principles of Gestalt Psychology (New York: Harcourt Brace and Company).
23. Kardos, L. (1934). Ding und Schatten: Eine experimentelle Untersuchung über die Grundlagen des Farbensehens. Z. Psychol. Z. Angew. Psychol. *23*, 1–184.
24. Jameson, D., and Hurvich, L.M. (1972). Sensitivity, contrast, and afterimages. In Visual Psychophysics (Handbook of Sensory Physiology), D. Jameson and L.M. Hurvich, eds. (Berlin: Springer-Verlag), pp. 568–581.
25. Geisler, W.S. (1978). Adaptation, afterimages and cone saturation. Vision Res. *18*, 279–289.
26. Adelson, E.H. (1982). Saturation and adaptation in the rod system. Vision Res. *22*, 1299–1312.
27. Walraven, J. (1976). Discounting the background—the missing link in the explanation of chromatic induction. Vision Res. *16*, 289–295.
28. Shevell, S.K. (1978). The dual role of chromatic backgrounds in color perception. Vision Res. *18*, 1649–1661.
29. Chubb, C., Sperling, G., and Solomon, J.A. (1989). Texture interactions determine perceived contrast. Proc. Natl. Acad. Sci. USA *86*, 9631–9635.
30. Victor, J.D., Conte, M.M., and Purpura, K.P. (1997). Dynamic shifts of the contrast-response function. Vis. Neurosci. *14*, 577–587.
31. Chander, D., and Chichilnisky, E.J. (2001). Adaptation to temporal contrast in primate and salamander retina. J. Neurosci. *21*, 9904–9916.
32. Solomon, S.G., Peirce, J.W., Dhruv, N.T., and Lennie, P. (2004). Profound contrast adaptation early in the visual pathway. Neuron *42*, 155–162.
33. Manookin, M.B., and Demb, J.B. (2006). Presynaptic mechanism for slow contrast adaptation in mammalian retinal ganglion cells. Neuron *50*, 453–464.
34. Heeger, D.J. (1992). Normalization of cell responses in cat striate cortex. Vis. Neurosci. *9*, 181–197.
35. Foley, J.M. (1994). Human luminance pattern-vision mechanisms: masking experiments require a new model. J. Opt. Soc. Am. A Opt. Image Sci. Vis. *11*, 1710–1719.
36. Blakeslee, B., and McCourt, M.E. (2004). A unified theory of brightness contrast and assimilation incorporating oriented multiscale spatial filtering and contrast normalization. Vision Res. *44*, 2483–2503.
37. DiCarlo, J.M., and Wandell, B.A. (2000). Rendering high dynamic range scenes. In Sensors and Camera Systems for Scientific, Industrial, and Digital Photography Applications, Proceedings of the SPIE, *Volume 3965*, M.M. Blouke, N. Sampat, G.M. Williams, Jr., and T. Yeh, eds. (Bellingham, WA: SPIE), pp. 392–401.
38. Reinhard, E., Ward, G., Pattanaik, S., and Debevec, P. (2006). High Dynamic Range Imaging (San Francisco: Elsevier).
39. Stiles, W.S. (1967). Mechanism concepts in colour theory. J. Colour Group *11*, 106–123.
40. Krantz, D. (1968). A theory of context effects based on cross-context matching. J. Math. Psychol. *5*, 1–48.
41. Brainard, D.H., and Wandell, B.A. (1992). Asymmetric color matching: how color appearance depends on the illuminant. J. Opt. Soc. Am. A *9*, 1433–1448.
42. Brainard, D.H., and Maloney, L.T. (2011). Surface color perception and equivalent illumination models. J. Vis. *11*, 1–18.
43. Seetzen, H., Heidrich, W., Stuezlinger, W., Ward, G., Whitehead, L., Trentacost, M., Ghosh, A., and Vorozcovs, A. (2004). High dynamic range display systems. ACM Trans. Graph. *23*, 760–768.
44. Radonjić, A., Broussard, C., and Brainard, D.H. (2011). Characterizing and controlling the spectral output of an HDR display. Brainard Lab Technical Report 2011-1, Department of Psychology, University of Pennsylvania, http://color.psych.upenn.edu/brainard/papers/hdrcharacterize.pdf.